A&A 622, A167 (2019)
https://doi.org/10.1051/0004-6361/201834696

Astronomy & Astrophysics

Theoretical investigation of energy levels and transition data for P II*

P. Rynkun[1], L. Radžiūtė[1], G. Gaigalas[1], and P. Jönsson[2]

[1] Institute of Theoretical Physics and Astronomy, Vilnius University, Saulėtekio av. 3, 10222 Vilnius, Lithuania
e-mail: pavel.rynkun@tfai.vu.lt
[2] Group for Materials Science and Applied Mathematics, Malmö University, 20506 Malmö, Sweden

Received 21 November 2018 / Accepted 2 January 2019

ABSTRACT

Aims. The main goal of this paper is to present accurate and extensive transition data for the P II ion. These data are useful in various astrophysical applications.
Methods. The multiconfiguration Dirac–Hartree–Fock (MCDHF) and relativistic configuration interaction (RCI) methods, which are implemented in the general-purpose relativistic atomic structure package GRASP2K, were used in the present work. In the RCI calculations the transverse-photon (Breit) interaction, the vacuum polarization, and the self-energy corrections were included.
Results. Energy spectra are presented for 48 even states of the $3s^23p^2$, $3s^23p\{4p, 4f, 5p, 5f, 6p\}$, $3s3p^23d$ configurations, and for 58 odd states of the $3s3p^3$, $3s^23p\{3d, 4s, 4d, 5s, 5d, 6s\}$ configurations in the P II ion. Electric dipole (E1) transition data are computed between these states along with the corresponding lifetimes. The average uncertainty of the computed transition energies is between five and ten times smaller than the uncertainties from previous calculations. The computed lifetimes for the $3s^23p4s\ ^3P^o$ states are within the error bars of the most current experimental values.

Key words. atomic data – radiative transfer

1. Introduction

P II is the dominant ion of the ionized phosphorus elements in the neutral interstellar medium. Singly ionized phosphorus has one of the strongest transitions at 1153 Å ($3s^23p^2\ ^3P$ – $3s^23p4s\ ^3P^o$) which is typically used to derive phosphorus abundances (Federman et al. 2007). Accurate transition data of P II are useful in astrophysical environments; they are important for the determination of column densities and velocity structure of the interstellar and intergalactic matter (Tayal 2003) .

Hibbert (1988) used configuration interaction as implemented in the CIV3 code to compute energy spectra and probabilities of electric dipole transitions. Tayal (2003) used the multiconfiguration Hartree–Fock (MCHF) method including relativistic corrections through the Breit–Pauli Hamiltonian to calculate energy spectra and transition data for allowed and intercombination lines. Fischer et al. (2006) computed energy levels of the $3s^23p^2$, $3s3p^3$, $3s^23p3d$, $3s^23p4s$, and $3s^23p4p$ configurations and transition data using MCHF with the Breit–Pauli approximation for including relativistic corrections. El-Maaref et al. (2012) calculated energy levels, and transition data of silicon-like ions P II, S III, Cl IV, Ar V, and K VI using CIV3. Cashman et al. (2017) compiled the atomic data that are of interest for astrophysics, focusing on the transitions of those ions that have been observed in the Milky Way interstellar medium and/or other galaxies.

Miller et al. (1971) presented the absolute transition probabilities of P I and P II lines measured using the shock-tube technique. Svendenius et al. (1983) measured lines of the P II spectrum in the wavelength region 500–12 000 Å. Federman et al. (2007) presented beam-foil measurements of lifetimes, oscillator strengths, and branching fractions for the multiplet ($3s^23p^2\ ^3P$ – $3s^23p4s\ ^3P^o$) transitions at 1154 Å.

In this work energy spectrum calculations were performed for 48 even states of the $3s^23p^2$, $3s^23p4p$, $3s^23p4f$, $3s^23p5p$, $3s^23p5f$, $3s^23p6p$, and $3s3p^23d$ configurations, and for 58 odd states of the $3s3p^3$, $3s^23p3d$, $3s^23p4s$, $3s^23p4d$, $3s^23p5s$, $3s^23p5d$, and $3s^23p6s$ configurations in P II. Furthermore, electric dipole (E1) transition data were computed between these states.

The calculations were done using multiconfiguration Dirac–Hartree–Fock (MCDHF) and relativistic configuration interaction (RCI) methods (Grant 2007; Fischer et al. 2016), which are implemented in the general-purpose relativistic atomic structure package GRASP2K (Jönsson et al. 2013). In the RCI calculations the transverse-photon (Breit) interaction, the vacuum polarization, and the self-energy corrections were included.

2. Methods

2.1. Computational procedure

The MCDHF method used in the present work is based on the Dirac-Coulomb Hamiltonian

$$H_{\rm DC} = \sum_{i=1}^{N}\left(c\ \boldsymbol{\alpha}_i\cdot\boldsymbol{p}_i + (\beta_i - 1)c^2 + V_i^N\right) + \sum_{i>j}^{N}\frac{1}{r_{ij}}, \quad (1)$$

where V^N is the monopole part of the electron–nucleus Coulomb interaction, $\boldsymbol{\alpha}$ and β are the 4×4 Dirac matrices, and c is the speed

* Table 5 is only available at the CDS via anonymous ftp to cdsarc.u-strasbg.fr (130.79.128.5) or via http://cdsarc.u-strasbg.fr/viz-bin/qcat?J/A+A/622/A167

Table 1. Summary of active space construction.

MR set		N_{CSFs}	
Even	Odd	Even	Odd
RCI			
$3s^23p^2$, $3s^23p4p$, $3s^23p4f$, $3s^23p5p$, $3s^23p5f$, $3s^23p6p$, $3p^4$, $3p^34p$, $3p^34f$, $3p^35p$, $3p^35f$, $3p^36p$	$3s3p^3$, $3s^23p3d$, $3s^23p4s$, $3s^23p4d$, $3s^23p5s$, $3s^23p5d$, $3s^23p6s$, $3s^23p6d$, $3s^23p7s$, $3p^33d$, $3p^34s$, $3p^34d$, $3p^35s$, $3p^35d$, $3p^36s$, $3p^36d$, $3p^37s$	799 548	787 578
RCI (CV) additionally included configurations			
$3s3p^23d$, $3s^23d^2$, $3s^23d7d$, $3s3p^27d$	$3s3p^24p$, $3p^37d$, $3s^23p7d$	5 954 032	4 815 663

of light in atomic units. The atomic state functions (ASFs) were obtained as linear combinations of symmetry adapted configuration state functions (CSFs)

$$\Psi(\gamma PJM) = \sum_{i=1}^{N_{\mathrm{CSFs}}} c_i \Phi(\gamma_i PJM). \tag{2}$$

Here J and M are the angular quantum numbers and P is parity. γ_i denotes other appropriate labeling of the configuration state function i, for example orbital occupancy and coupling scheme. Normally the label γ of the atomic state function is the same as the label of the dominating CSF. The CSFs are built from products of one-electron Dirac orbitals. Based on a weighted energy average of several states, the so-called extended optimal level (EOL) scheme (Dyall et al. 1989), both the radial parts of the Dirac orbitals, and the expansion coefficients were optimized to self-consistency in the relativistic self-consistent field procedure.

In subsequent RCI calculations the transverse photon interaction (Breit interaction),

$$H_{\mathrm{Breit}} = -\sum_{i<j}^{N} \left[\boldsymbol{\alpha}_i \cdot \boldsymbol{\alpha}_j \frac{\cos(\omega_{ij} r_{ij}/c)}{r_{ij}} + (\boldsymbol{\alpha}_i \cdot \boldsymbol{\nabla}_i)(\boldsymbol{\alpha}_j \cdot \boldsymbol{\nabla}_j) \frac{\cos(\omega_{ij} r_{ij}/c) - 1}{\omega_{ij}^2 r_{ij}/c^2} \right], \tag{3}$$

was included in the Hamiltonian. The photon frequencies ω_{ij}, used for calculating the matrix elements of the transverse photon interaction, were taken as the difference of the diagonal Lagrange multipliers associated with the Dirac orbitals (McKenzie et al. 1980). In the RCI calculation the leading quantum electrodynamics corrections (QED), self-interaction and vacuum polarization, were also included.

In the present calculations, the ASFs were obtained as expansions over jj-coupled CSFs. To provide the LSJ labeling system, the ASFs were transformed from a jj-coupled CSF basis into an LSJ-coupled CSF basis using the method provided by Gaigalas et al. (2003, 2017).

2.2. Computation of transition parameters

The transition data (transition probabilities, oscillator strengths) between two states $\gamma' P' J' M'$ and γPJM can be expressed in terms of the transition moment, which is defined as

$$\langle \Psi(\gamma PJ) \| \mathbf{T} \| \Psi(\gamma' P' J') \rangle = \sum_{j,k} c_j c'_k \langle \Phi(\gamma_j PJ) \| \mathbf{T} \| \Phi(\gamma'_k P' J') \rangle, \tag{4}$$

where $\mathbf{T}$ is the transition operator. For electric dipole and quadrupole (E1 and E2) transitions there are two forms of the transition operator: the length (Babushkin) and velocity (Coulomb) forms, which for the exact solutions of the Dirac-equation give the same value of the transition moment (Grant 1974). The quantity dT, characterizing the uncertainty of the computed transition rates, is defined as

$$dT = \frac{|A_{\mathrm{l}} - A_{\mathrm{v}}|}{\max(A_{\mathrm{l}}, A_{\mathrm{v}})}, \tag{5}$$

where A_{l} and A_{v} are transition rates in length and velocity forms.

The calculation of the transition moment breaks down to the task of summing up reduced matrix elements between different CSFs.

3. Scheme of calculations

As a starting point, MCDHF calculations were performed in the extended optimal level scheme for the weighted average of the even and odd parity states simultaneously. The ASFs were constructed using the multireference-single-double (MR-SD) method (Fischer et al. 2016). The MR sets for the even and odd parities are presented in the Table 1, which also displays the number of CSFs in the final even and odd state expansions distributed over the different J symmetries.

The CSF expansions were obtained by allowing SD substitutions from the configurations in the MR to active orbital sets $\{12s, 11p, 11d, 10f, 9g, 7h, 7i\}$. Only CSFs that have nonzero matrix elements with the CSFs belonging to the configurations in the MR were retained. No substitutions were allowed from the 1s, 2s, 2p shells, which defines an inactive closed core. The MCDHF calculations were followed by RCI calculations, done separately for even and odd states. At the last step, MR was extended and core-valence (CV) correlation (the single substitutions from 2p shell was allowed) was included in the RCI calculations. Single substitutions from 2p shell were allowed to active orbital sets $\{9s, 8p, 8d, 7f, 6g\}$.

4. Results

In the present work, energy spectra are presented for the 106 (48 even, and 58 odd) lowest states in P II.

To evaluate the accuracy, the obtained transition energies are compared with results from the NIST (Kramida et al. 2018) database, and other theoretical computations (Fig. 1). The figure

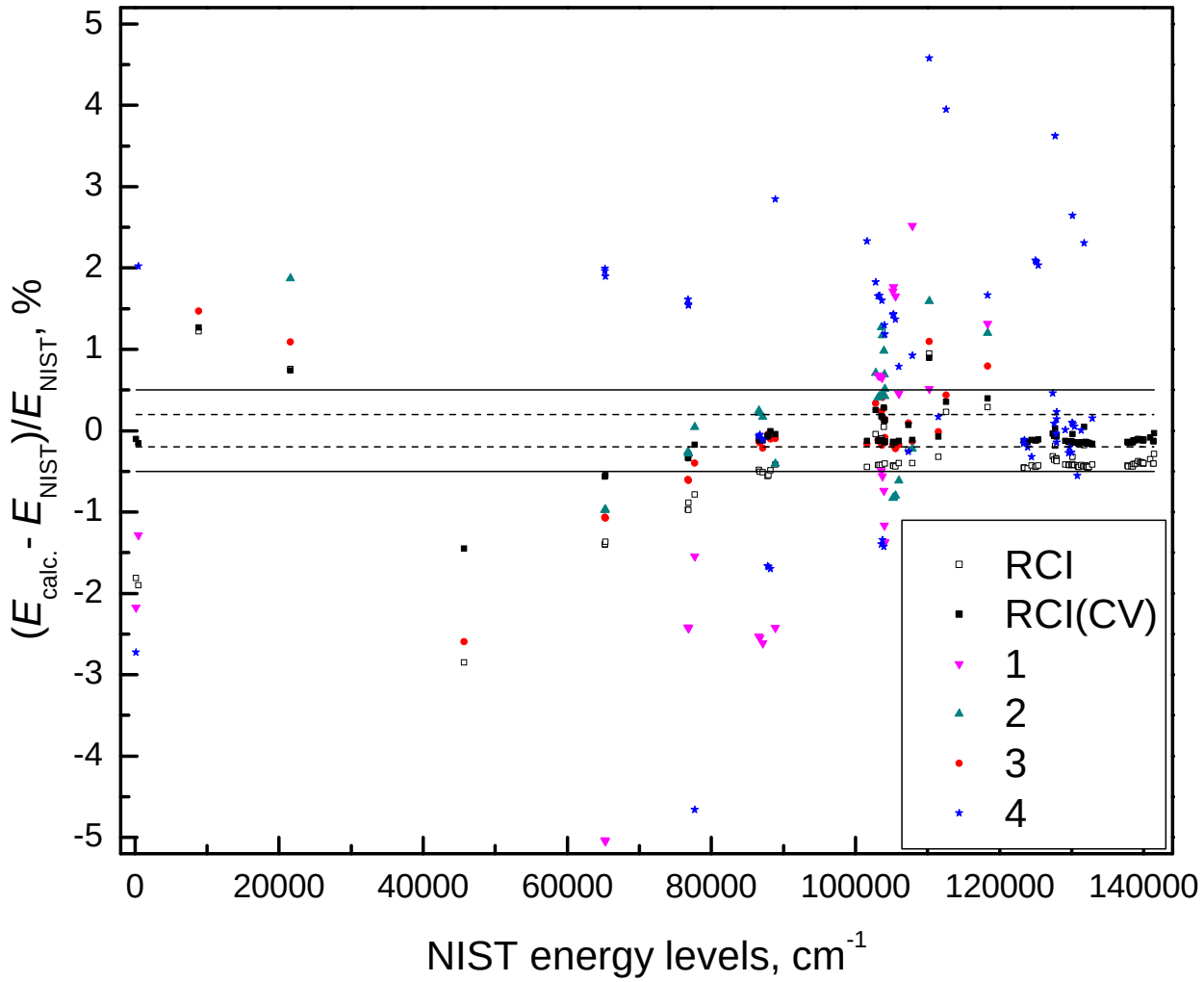

Fig. 1. Comparison of computed energy levels in present work and other theoretical results with data from NIST database. The dashed and solid lines indicate the 0.2% and 0.5% deviations, respectively. (1) Hibbert (1988); (2) Tayal (2003); (3) Fischer et al. (2006); (4) El-Maaref et al. (2012).

Table 2. Comparison of computed energy levels in present work and other theoretical results with data from NIST database.

Av. accuracy (in %)	No. of levels in Ref.	Ref.
0.19	97	RCI (CV)
2.95	31	1
1.65	32	2
1.08	40	3
1.27	63	4

References. (1) Hibbert (1988); (2) Tayal (2003); (3) Fischer et al. (2006); (4) El-Maaref et al. (2012).

Table 3. Comparison of computed lifetimes (in ns) for $3s^2 3p 4s\ ^3P^o$ states of P II ion.

$J = 0$	$J = 1$	$J = 2$	Ref.
0.802(0.26)	0.795(0.35)	0.786(0.35)	RCI (CV)
0.82	0.81	0.80	1
0.784	0.778	0.772	2
0.796	0.789	0.776	3
0.785	0.782	0.775	4
		0.80	5
0.79 ± 0.10	0.79 ± 0.06	0.84 ± 0.07	6 (Exp.)
0.85 ± 0.11	0.85 ± 0.11	0.85 ± 0.11	7 (Exp.)
1.3 ± 0.5	1.3 ± 0.5	1.3 ± 0.5	8 (Exp.)

Notes. Lifetimes of present calculations are given in length form. The estimated uncertainty on the lifetime is given as a percentage in parentheses.

References. (1) Hibbert (1988); (2) Tayal (2003); (3) Fischer et al. (2006); (4) El-Maaref et al. (2012); (5) Brage et al. (1993); (6) Federman et al. (2007); (7) Livingston et al. (1975); (8) Smith (1978).

also shows the contributions from core-valence electron correlations and extensions of the MR sets in the present calculations. The final result (RCI (CV)) for the energy spectra agrees very well with NIST. The disagreement is up to 0.15%, except for a few less-excited states where it reaches 1.5%. The averaged uncertainty of computed energy spectra comparing with NIST data is 0.19%. Comparing with other calculations it is seen from Fig. 1 that the results of Fischer et al. (2006) also agree well with the NIST, but the authors calculated less energy levels (41 levels). In Fischer et al. (2006) the largest disagreement is by about 13% for $3s^2 3p^2(^3_2P)\ ^3P_{1,2}$ states (these points were not included in the Fig. 1). In Table 2 a summary of previous calculations is presented: namely, the number of computed energy levels (No. of levels in Ref.) and the average percentage difference between

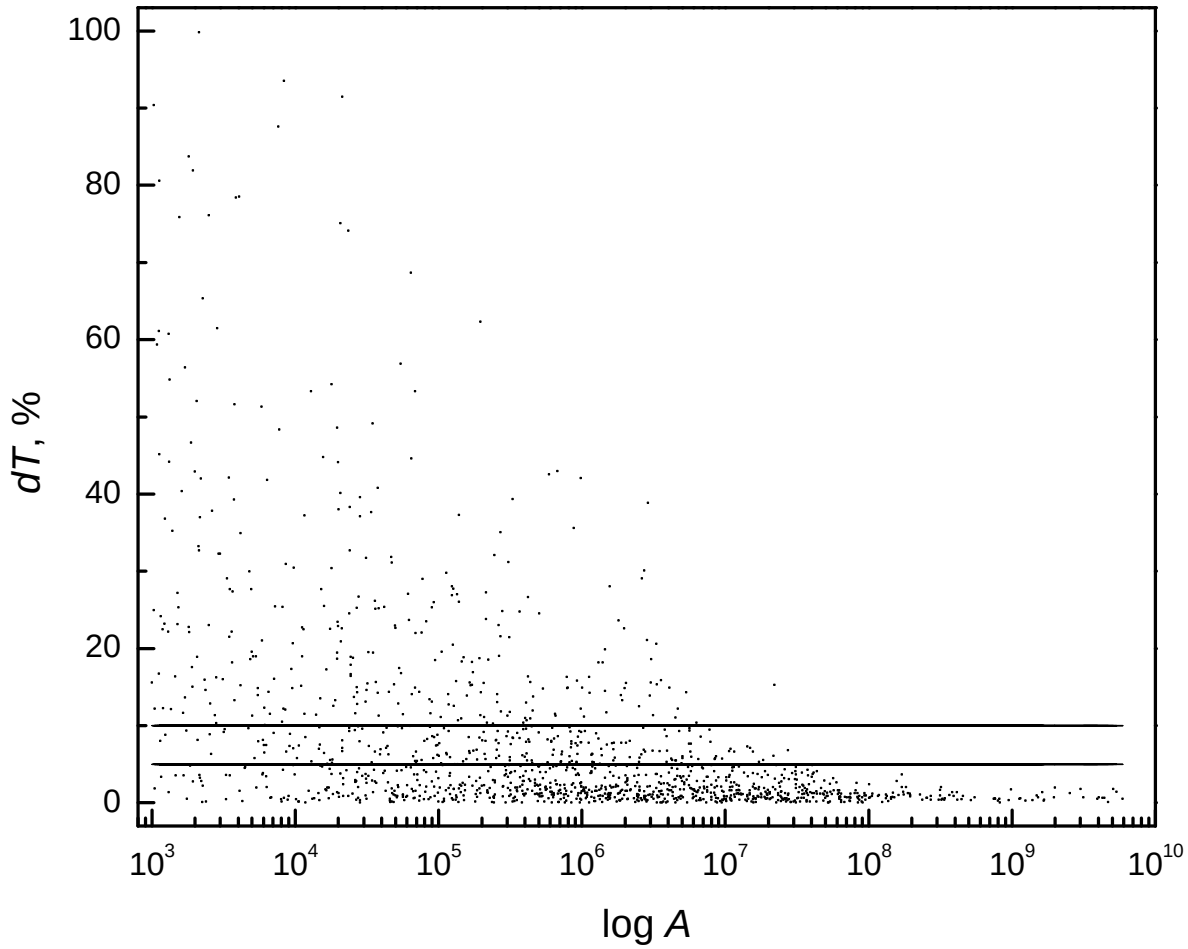

Fig. 2. Scatterplot of dT: the relative difference between the transition rates in length and velocity form vs. the transition rate A for P II. The solid lines indicate the 5% and 10% deviations.

Table 4. Comparison of wavelengths and oscillator strengths for the $3s^2\,3p^2(^3_2P)\,^3P \rightarrow 3s^2\,3p\,^2P\,4s\,^3P^o$ transitions in P II.

$J_i \rightarrow J_f$						Ref.
$1 \rightarrow 2$	$0 \rightarrow 1$	$2 \rightarrow 2$	$1 \rightarrow 1$	$1 \rightarrow 0$	$2 \rightarrow 1$	
$f \times 10^{-2}$						
10.66 (0.4)	24.97 (0.4)	19.00 (0.3)	6.19 (0.4)	8.36 (0.3)	6.27 (0.3)	RCI (CV)
10.4	24.4	18.6	6.1	8.1	6.2	1
10.8	25.1	19.2	6.20	8.48	6.30	2
10.82	25.30	19.26	6.26	8.42	6.34	3
7.8	19.0	14.0	4.7	6.2	4.7	4
10.5 ± 1.1	27.2 ± 2.9	17.4 ± 1.6	6.4 ± 0.6	8.5 ± 1.1	5.9 ± 0.6	5 (Exp.)
λ (in Å)						
1151.34	1154.25	1155.38	1156.45	1158.13	1160.53	RCI (CV)
1152.18	1154.59	1155.68	1156.51	1158.26	1160.04	3
1170.41	1172.64	1174.83	1174.88	1177.12	1179.32	4
1149.958	1152.818	1153.995	1155.014	1156.970	1159.086	5 (Exp.)

Notes. The oscillator strengths in the RCI column are given in the length gauge. The estimated uncertainty on the oscillator strengths is given as a percentage in parentheses.
References. (1) Hibbert (1988); (2) Tayal (2003); (3) Fischer et al. (2006); (4) El-Maaref et al. (2012); (5) Federman et al. (2007).

NIST and the different methods for the states covered by these methods (Av. accuracy). Final results (RCI (CV)) of energy spectra and lifetimes in length and velocity forms obtained from E1 transitions are displayed in Table A.1. In the present work states of $3s3p^23d$ and $3s^23p6p$ configurations are presented for the first time.

Lifetimes for $3s^23p4s\ ^3P^o$ states are compared with experiment and other theoretical calculations in Table 3. Computed

lifetimes are within the uncertainties of experimental measurement.

Transition data such as wavelengths, weighted oscillator strengths, transition rates of E1 transitions and the accuracy indicator dT are given in Table 5, available at the CDS. Generally, the uncertainty of transition data is small for the stronger transitions. To display this, a scatterplot of dT vs. the transition rate A for computed E1 transitions (with $A > 1000\,\mathrm{s}^{-1}$) is given in Fig. 2. For most of the strongest transitions, dT is well below 2%. The mean dT for all presented transitions is 7.83%. Table 4 displays the comparison of the theoretical and experimental results of wavelengths and oscillator strengths for the $3s^2\,3p^2(^3_2P)\ ^3P \rightarrow 3s^2\,3p\ ^2P\,4s\ ^3P^o$ transition. From the table we see that there is very good agreement between wavelengths and oscillator strengths computed in this work and the experimental values (Federman et al. 2007).

5. Conclusions

In the present work energy spectra are computed for the 106 lowest states in P II using MCDHF and RCI methods. The mean uncertainty of calculated energy levels comparing with NIST data is 0.19%. The states of $3s3p^23d$ and $3s^23p6p$ configurations are presented for the first time.

Transition data for E1 transitions between computed states are presented. For most of the strongest transitions, dT is well below 2%. Lifetimes obtained from E1 transitions are also presented.

Acknowledgements. This research was funded by a grant (No. S-LJB- 18-1) from the Research Council of Lithuania.

References

Brage, T., Merkelis, G., & Fischer, C. F. 1993, Phys. Lett. A, 174, 111
Cashman, F. H., Kulkarni, V. P., Kisielius, R., Ferland, G. J., & Bogdanovich, P. 2017, ApJS, 230, 8
Dyall, K., Grant, I., Johnson, C., Parpia, F., & Plummer, E. 1989, Comput. Phys. Commun., 55, 425
El-Maaref, A. A., Uosif, M., Allam, S., & El-Sherbini, T. 2012, At. Data Nucl. Data Tab., 98, 589
Federman, S. R., Brown, M., Torok, S., et al. 2007, ApJ, 660, 919
Fischer, C. F., Tachiev, G., & Irimia, A. 2006, At. Data Nucl. Data Tab., 92, 607
Fischer, C. F., Godefroid, M., Brage, T., Jönsson, P., & Gaigalas, G. 2016, J. Phys. B At. Mol. Opt. Phys., 49, 182004
Gaigalas, G., Žalandauskas, T., & Rudzikas, Z. 2003, At. Data Nucl. Data Tab., 84, 99
Gaigalas, G., Fischer, C., Rynkun, P., & Jönsson, P. 2017, Atoms, 5, 6
Grant, I. P. 1974, J. Phys. B At. Mol. Opt. Phys., 7, 1458
Grant, I. P. 2007, Relativistic Quantum Theory of Atoms and Molecules (New York: Springer)
Hibbert, A. 1988, Phys. Scr., 38, 37
Jönsson, P., Gaigalas, G., Bieroń, J., Fischer, C. F., & Grant, I. 2013, Comput. Phys. Commun., 184, 2197
Kramida, A., Ralchenko, Yu., Reader, J., & NIST ASD Team 2018, NIST Atomic Spectra Database (ver. 5.5.6), https://physics.nist.gov/asd, National Institute of Standards and Technology, Gaithersburg, MD
Livingston, A. E., Kernahan, J. A., Irwin, D. J. G., & Pinnington, E. H. 1975, Phys. Scr., 12, 223
McKenzie, B., Grant, I., & Norrington, P. 1980, Comput. Phys. Commun., 21, 233
Miller, M. H., Roig, R. A., & Bengtson, R. D. 1971, Phys. Rev. A, 4, 1709
Smith, W. H. 1978, Phys. Scr., 17, 513
Svendenius, N., Magnusson, C. E., & Zetterberg, P. O. 1983, Phys. Scr., 27, 339
Tayal, S. S. 2003, ApJS, 146, 459

Appendix A: Computed energy levels and lifetimes for the P II ion

Table A.1. Computed energy levels (in cm^{-1}) and lifetimes (in s) in length and velocity gauges for the P II ion.

No.	Label	RCI (CV)	NIST	τ_l	τ_v
1	$3s^2\,3p^2(^3_2P)\,^3P_0$	0	0		
2	$3s^2\,3p^2(^3_2P)\,^3P_1$	164	165		
3	$3s^2\,3p^2(^3_2P)\,^3P_2$	468	469		
4	$3s^2\,3p^2(^1_2D)\,^1D_2$	8994	8882		
5	$3s^2\,3p^2(^1_0S)\,^1S_0$	21 735	21 576		
6	$3s\,3p^3(^4_3S)\,^5S^o_2$	45 035	45 697	1.78E-04	1.50E-04
7	$3s\,3p^3(^2_3D)\,^3D^o_1$	64 881	65 251	9.13E-08	8.61E-08
8	$3s\,3p^3(^2_3D)\,^3D^o_2$	64 903	65 272	9.23E-08	8.68E-08
9	$3s\,3p^3(^2_3D)\,^3D^o_3$	64 947	65 307	9.34E-08	8.71E-08
10	$3s\,3p^3(^2_1P)\,^3P^o_2$	76 504	76 764	1.33E-08	1.29E-08
11	$3s\,3p^3(^2_1P)\,^3P^o_1$	76 552	76 812	1.23E-08	1.19E-08
12	$3s\,3p^3(^2_1P)\,^3P^o_0$	76 596	76 823	1.21E-08	1.18E-08
13	$3s^2\,3p\,^2P\,3d\,^1D^o_2$	77 572	77 710	2.05E-07	1.88E-07
14	$3s^2\,3p\,^2P\,4s\,^3P^o_0$	86 510	86 598	8.02E-10	7.99E-10
15	$3s^2\,3p\,^2P\,4s\,^3P^o_1$	86 636	86 744	7.95E-10	7.92E-10
16	$3s^2\,3p\,^2P\,4s\,^3P^o_2$	87 019	87 125	7.86E-10	7.84E-10
17	$3s^2\,3p\,^2P\,3d\,^3F^o_2$	87 741	87 804	3.20E-06	3.18E-06
18	$3s^2\,3p\,^2P\,3d\,^3F^o_3$	87 918	87 967	1.48E-06	1.51E-06
19	$3s^2\,3p\,^2P\,3d\,^3F^o_4$	88 182	88 192		
20	$3s^2\,3p\,^2P\,4s\,^1P^o_1$	88 851	88 893	6.65E-10	6.63E-10
21	$3s^2\,3p\,^2P\,4p\,^1P_1$	101 508	101 636	1.18E-08	1.17E-08
22	$3s^2\,3p\,^2P\,4p\,^3D_1$	103 035	103 166	1.00E-08	9.97E-09
23	$3s^2\,3p\,^2P\,3d\,^1P^o_1$	103 059	102 798	4.69E-10	4.67E-10
24	$3s^2\,3p\,^2P\,4p\,^3D_2$	103 211	103 339	9.95E-09	9.88E-09
25	$3s^2\,3p\,^2P\,4p\,^3D_3$	103 547	103 668	9.91E-09	9.83E-09
26	$3s^2\,3p\,^2P\,3d\,^3P^o_2$	103 809	103 630	2.15E-10	2.14E-10
27	$3s^2\,3p\,^2P\,3d\,^3D^o_1$	103 911	104 054	1.98E-10	1.97E-10
28	$3s^2\,3p\,^2P\,3d\,^3D^o_3$	104 174	104 050	1.69E-10	1.69E-10
29	$3s^2\,3p\,^2P\,3d\,^3P^o_1$	104 204	103 756	2.12E-10	2.10E-10
30	$3s^2\,3p\,^2P\,3d\,^3P^o_0$	104 231	103 940	2.53E-10	2.51E-10
31	$3s^2\,3p\,^2P\,3d\,^3D^o_2$	104 234	104 102	1.93E-10	1.92E-10
32	$3s^2\,3p\,^2P\,4p\,^3P_0$	105 075	105 224	6.67E-09	6.66E-09
33	$3s^2\,3p\,^2P\,4p\,^3P_1$	105 148	105 302	6.72E-09	6.71E-09
34	$3s^2\,3p\,^2P\,4p\,^3P_2$	105 396	105 550	6.66E-09	6.65E-09
35	$3s^2\,3p\,^2P\,4p\,^3S_1$	105 864	106 001	7.53E-09	7.52E-09
36	$3s^2\,3p\,^2P\,3d\,^1F^o_3$	107 436	107 360	2.13E-10	2.13E-10
37	$3s^2\,3p\,^2P\,4p\,^1D_2$	107 800	107 923	8.65E-09	8.59E-09
38	$3s\,3p^3(^4_3S)\,^3S^o_1$	111 237	110 255	1.10E-10	1.08E-10
39	$3s^2\,3p\,^2P\,4p\,^1S_0$	111 427	111 508	7.92E-09	7.84E-09
40	$3s\,3p^3(^2_3D)\,^1D^o_2$	113 006	112 607	1.85E-10	1.83E-10
41	$3s\,3p^3(^2_1P)\,^1P^o_1$	118 808	118 342	2.20E-10	2.17E-10
42	$3s^2\,3p\,^2P\,5s\,^3P^o_0$	123 183	123 344	2.05E-09	2.05E-09
43	$3s^2\,3p\,^2P\,5s\,^3P^o_1$	123 277	123 455	2.01E-09	2.00E-09
44	$3s^2\,3p\,^2P\,5s\,^3P^o_2$	123 715	123 891	1.97E-09	1.97E-09
45	$3s^2\,3p\,^2P\,5s\,^1P^o_1$	124 286	124 432	1.68E-09	1.68E-09
46	$3s^2\,3p\,^2P\,4d\,^3F^o_2$	124 792	124 947	4.80E-09	4.84E-09
47	$3s^2\,3p\,^2P\,4d\,^3F^o_3$	124 979	125 129	4.88E-09	4.93E-09
48	$3s^2\,3p\,^2P\,4d\,^3F^o_4$	125 254	125 391	5.14E-09	5.21E-09
49	$3s^2\,3p\,^2P\,4d\,^3P^o_2$	127 318	127 367	6.97E-10	6.92E-10
50	$3s^2\,3p\,^2P\,4d\,^3D^o_1$	127 509	127 599	6.62E-10	6.59E-10

Notes. Energy levels are given relative to a ground state energy.

Table A.1. continued.

No.	Label	RCI (CV)	NIST	τ_l	τ_v
51	$3s^2\,3p\,^2P\,4d\,^1D^o_2$	127 789	127 756	4.26E-10	4.21E-10
52	$3s^2\,3p\,^2P\,4d\,^3D^o_3$	127 812	127 888	5.40E-10	5.38E-10
53	$3s^2\,3p\,^2P\,4d\,^3P^o_0$	127 828	127 900	1.03E-09	1.03E-09
54	$3s^2\,3p\,^2P\,4d\,^3P^o_1$	127 838	127 934	7.60E-10	7.56E-10
55	$3s^2\,3p\,^2P\,4d\,^3D^o_2$	127 867	127 950	6.21E-10	6.17E-10
56	$3s^2\,3p\,^2P\,5p\,^1P_1$	128 944	129 110	1.96E-08	2.05E-08
57	$3s^2\,3p\,^2P\,5p\,^3D_1$	129 390	129 569	2.48E-08	2.59E-08
58	$3s^2\,3p\,^2P\,5p\,^3D_2$	129 484	129 665	2.61E-08	2.73E-08
59	$3s^2\,3p\,^2P\,5p\,^3D_3$	129 847	130 020	2.67E-08	2.80E-08
60	$3s^2\,3p\,^2P\,5p\,^3P_0$	129 872	130 058	1.42E-08	1.49E-08
61	$3s^2\,3p\,^2P\,5p\,^3P_1$	129 983	130 173	1.52E-08	1.58E-08
62	$3s^2\,3p\,^2P\,4d\,^1F^o_3$	130 081	130 143	5.52E-10	5.53E-10
63	$3s^2\,3p\,^2P\,5p\,^3P_2$	130 210	130 400	1.48E-08	1.55E-08
64	$3s^2\,3p\,^2P\,5p\,^3S_1$	130 603	130 801	2.10E-08	2.19E-08
65	$3s^2\,3p\,^2P\,4f\,^1F_3$	130 713	130 913	2.93E-09	2.98E-09
66	$3s^2\,3p\,^2P\,4f\,^3F_2$	130 744	130 949	3.15E-09	3.21E-09
67	$3s^2\,3p\,^2P\,4f\,^3F_3$	130 791	130 993	3.06E-09	3.11E-09
68	$3s^2\,3p\,^2P\,4f\,^3F_4$	130 827	131 025	3.16E-09	3.22E-09
69	$3s^2\,3p\,^2P\,5p\,^1D_2$	131 162	131 352	1.85E-08	1.93E-08
70	$3s^2\,3p\,^2P\,4f\,^3G_3$	131 431	131 631	3.01E-09	3.04E-09
71	$3s^2\,3p\,^2P\,4f\,^3G_4$	131 494	131 689	3.22E-09	3.27E-09
72	$3s^2\,3p\,^2P\,4f\,^3G_5$	131 757	131 940	3.02E-09	3.07E-09
73	$3s^2\,3p\,^2P\,4d\,^1P^o_1$	131 822	131 763	4.46E-10	4.41E-10
74	$3s^2\,3p\,^2P\,4f\,^1G_4$	131 886	132 078	4.13E-09	4.20E-09
75	$3s^2\,3p\,^2P\,4f\,^3D_3$	131 922	132 132	3.42E-09	3.44E-09
76	$3s^2\,3p\,^2P\,4f\,^3D_2$	131 950	132 163	3.81E-09	3.84E-09
77	$3s^2\,3p\,^2P\,4f\,^3D_1$	132 161	132 372	3.44E-09	3.46E-09
78	$3s^2\,3p\,^2P\,4f\,^1D_2$	132 192	132 397	3.86E-09	3.89E-09
79	$3s^2\,3p\,^2P\,5p\,^1S_0$	132 685	132 901	1.91E-08	1.94E-08
80	$3s^2\,3p\,^2P\,6s\,^3P^o_0$	137 568	137 757	4.21E-09	4.25E-09
81	$3s^2\,3p\,^2P\,6s\,^3P^o_1$	137 621	137 827	3.90E-09	3.92E-09
82	$3s\,3p^2(^3_2P)\,^4P\,3d\,^5F_1$	137 861		1.44E-05	1.35E-05
83	$3s\,3p^2(^3_2P)\,^4P\,3d\,^5F_2$	137 923		1.42E-05	1.42E-05
84	$3s\,3p^2(^3_2P)\,^4P\,3d\,^5F_3$	138 027		1.61E-05	1.83E-05
85	$3s^2\,3p\,^2P\,6s\,^3P^o_2$	138 108	138 309	3.98E-09	4.00E-09
86	$3s\,3p^2(^3_2P)\,^4P\,3d\,^5F_4$	138 171		2.23E-05	2.55E-05
87	$3s^2\,3p\,^2P\,6s\,^1P^o_1$	138 322	138 522	3.08E-09	3.07E-09
88	$3s\,3p^2(^3_2P)\,^4P\,3d\,^5F_5$	138 381		8.80E-05	8.62E-05
89	$3s^2\,3p\,^2P\,5d\,^3F^o_2$	138 382	138 552	8.18E-09	8.34E-09
90	$3s^2\,3p\,^2P\,5d\,^3F^o_3$	138 575	138 743	8.43E-09	8.64E-09
91	$3s^2\,3p\,^2P\,5d\,^3F^o_4$	138 881	139 040	1.12E-08	1.16E-08
92	$3s\,3p^2(^3_2P)\,^4P\,3d\,^3P_2$	138 932		1.83E-08	1.77E-08
93	$3s^2\,3p\,^2P\,5d\,^1D^o_2$	139 072	139 213	1.79E-09	1.77E-09
94	$3s^2\,3p\,^2P\,5d\,^3D^o_1$	139 362	139 526	1.63E-09	1.62E-09
95	$3s^2\,3p\,^2P\,5d\,^3D^o_2$	139 469	139 623	1.81E-09	1.79E-09
96	$3s^2\,3p\,^2P\,5d\,^3D^o_3$	139 644	139 804	1.54E-09	1.53E-09
97	$3s^2\,3p\,^2P\,5d\,^3P^o_2$	139 754	139 924	2.02E-09	2.01E-09
98	$3s^2\,3p\,^2P\,5d\,^3P^o_1$	139 786	139 958	2.45E-09	2.43E-09
99	$3s^2\,3p\,^2P\,5d\,^3P^o_0$	139 815	139 971	2.88E-09	2.86E-09
100	$3s^2\,3p\,^2P\,6p\,^3D_2$	140 655		3.04E-08	3.37E-08
101	$3s^2\,3p\,^2P\,5d\,^1F^o_3$	140 831	140 950	1.18E-09	1.18E-09
102	$3s^2\,3p\,^2P\,6p\,^3D_3$	141 055		2.14E-08	2.28E-08
103	$3s^2\,3p\,^2P\,5f\,^1F_3$	141 141	141 325	6.19E-09	6.28E-09
104	$3s^2\,3p\,^2P\,5f\,^3F_3$	141 172	141 354	7.23E-09	7.41E-09
105	$3s^2\,3p\,^2P\,5f\,^3F_4$	141 184	141 370	6.58E-09	6.74E-09
106	$3s^2\,3p\,^2P\,5d\,^1P^o_1$	141 442	141 488	1.06E-09	1.05E-09